

An Efficient Method for Band Structure Calculations in 2D Photonic Crystals

David C. Dobson*

Department of Mathematics, Texas A&M University, College Station, Texas 77843-3368

E-mail: dobson@math.tamu.edu

Received August 25, 1998; revised November 11, 1998

An efficient method for band structure calculations in dielectric photonic crystals is presented. The method uses a finite element discretization coupled with a preconditioned subspace iteration algorithm. Numerical examples are presented which illustrate the behavior of the method. © 1999 Academic Press

1. INTRODUCTION

Photonic crystals are periodic structures composed of dielectric materials and designed to exhibit interesting properties, such as spectral band gaps, in the propagation of classical electromagnetic waves. Structures with band gaps have many potential applications, for example, in optical communications, filters, lasers, and microwaves. See [2, 13] for an introduction to photonic crystals. Figotin and Kuchment have proved that periodic dielectric structures exist which exhibit band gaps [9, 10], and other band gap structures have been found through computational and physical experiments. Computation has become a primary tool for investigating the properties of these structures.

Carrying out a complete band structure calculation for a given photonic crystal generally involves solving a large family of eigenproblems, as the *quasimomentum* parameter (defined in the next section) is varied over the first Brillouin zone. Solving this set of eigenproblems can be a computational burden, even for a single given photonic crystal. The computational cost is greatly multiplied in optimal design situations, where one wishes to evaluate a large number of structures in order to find one with some optimal property.

In this paper we describe a method which is well suited for efficient band structure calculations in photonic crystals. Here we consider only “two-dimensional” structures. The central building block of our approach is a subspace preconditioning method for general symmetric eigenproblems studied by Bramble, Knyazev, and Pasciak [3]. Our method

*Research supported by AFOSR Grant F49620-98-1-0005 and Alfred P. Sloan Research Fellowship.

combines the subspace preconditioning algorithm with a simple finite element discretization of the original family of eigenproblems, and a fast Fourier transform preconditioner. The subspace preconditioning algorithm is an iterative method which takes a given approximate eigen-subspace and iteratively improves it. This makes the method very efficient for solving continuously varying families of problems, as in band structure calculations. Small changes in the parameter generally result in small changes in the associated eigen-subspace, so that the subspace from a previous solve can be used as an accurate estimate for the next parameter value. Further efficiency is gained through the use of a preconditioner. Our preconditioner is most effective for structures composed of “low-contrast” mixtures of materials. In the optical frequency range, the contrast between the refractive indices k_1 , k_2 of two typical dielectric materials is generally relatively low (say $k_1/k_2 \leq 3$). In this parameter regime, the method is efficient enough to apply in an optimal design setting [5].

Many other methods have been developed for the computation of band structures in photonic crystals, both 2D and 3D. Most previous methods which allow for general dielectric structures are based on natural truncated plane wave decompositions of the fields (see, e.g., the survey [2] and the references therein). While acceptable accuracy can be obtained with these methods, it is often at a large computational cost, due to the slow convergence of the truncated field in media with sharp discontinuities. Alternative methods such as the T-matrix and R-matrix methods have been proposed and are based on calculating a transfer matrix for Maxwell’s equations. Such propagation methods are particularly useful for calculations in truncated structures. A comparison of the T-matrix and R-matrix approaches can be found in [7]. A method designed specifically for band structure calculations in certain crystal configurations which are known to produce band gaps has been developed by Figotin and Godin [8]. This method is highly efficient even for materials with large contrasts.

Finally, Axmann and Kuchment [1] have recently proposed a finite element method for band structure calculations in 2D photonic crystals. Their basic approach is similar to the method described here, but different in two main respects. First, their finite element approximation scheme uses general unstructured grids, where the method presented here uses a uniform, rectangular grid. Rectangular grids are easier to implement, but unstructured grids generally offer a more accurate field approximation using fewer grid points. The second main difference is the method of solution for the discrete eigenproblems. Our approach uses a fast approximate solution operator as a preconditioner, which is embedded within the subspace iterations, and which makes use of the fact that the grid is rectangular. Axmann and Kuchment use a simultaneous coordinate over-relaxation method, which does not require the use of an approximate solution operator. Each approach presents certain advantages and disadvantages; perhaps further work will produce new methods achieving the best features of both.

Extension of the finite element approach to the full Maxwell equations in 3D photonic crystals is work in progress. Finite element techniques for typical 3D electromagnetics problems in engineering are well developed [12]. Also, the efficiency of the solution methods described here and in [1] for 2D problems is very favorable for large problems. Our hope is that by coupling known 3D finite element discretization techniques with a fast solution algorithm, an effective method for 3D photonic crystals will result.

The outline of the remainder of this paper is as follows. In the following section, we formulate the discrete finite element problem. Then in Section 3, we introduce a fast Fourier transform (FFT) preconditioner. In Section 4, we describe the subspace preconditioning algorithm. Finally in Section 5 we numerically illustrate some of the properties of the method.

2. PROBLEM FORMULATION

Beginning with Maxwell's equations

$$\nabla \times E - i\omega\mu H = 0, \quad \nabla \times H + i\omega\epsilon E = 0, \tag{1}$$

we assume that the magnetic permeability μ is constant, and the medium is orthotropic, that is, the dielectric tensor ϵ can be written

$$\epsilon = \begin{pmatrix} \epsilon_{11} & \epsilon_{12} & 0 \\ \epsilon_{21} & \epsilon_{22} & 0 \\ 0 & 0 & \epsilon_{33} \end{pmatrix}. \tag{2}$$

We assume that all material properties are constant in the x_3 direction, that ϵ is positive definite, and that $\epsilon_{12} = \epsilon_{21}$. In the E -parallel case, where the electric field is given by $E = (0, 0, u)$, Eqs. (1) then reduce to

$$\Delta u + \omega^2 \rho u = 0, \quad \text{in } \mathbb{R}^2, \tag{3}$$

where $\rho(x) = \mu\epsilon_{33}(x)$, $x = (x_1, x_2)$. In the H -parallel case, where the magnetic field is given by $H = (0, 0, u)$, Eqs. (1) reduce to

$$\nabla \cdot (M\nabla u) + \omega^2 u = 0, \quad \text{in } \mathbb{R}^2, \tag{4}$$

where the matrix $M(x)$ is given by

$$M = \frac{1}{\mu(\epsilon_{11}\epsilon_{22} - \epsilon_{12}^2)} \begin{pmatrix} \epsilon_{22} & -\epsilon_{12} \\ -\epsilon_{12} & \epsilon_{11} \end{pmatrix}. \tag{5}$$

We assume that the structure has unit periodicity on a square lattice. Thus denoting $Z = \{0, \pm 1, \pm 2, \dots\}$, and defining the lattice $\Lambda = Z^2$, we assume that

$$\epsilon(x + n) = \epsilon(x), \quad \text{for all } x \in \mathbb{R}^2, \text{ and for all } n \in \Lambda.$$

We define the periodic domain

$$\Omega = \mathbb{R}^2 / Z^2,$$

which can be identified with the unit square $(0, 1)^2$ with periodic boundary conditions. Define the first Brillouin zone $K = [-\pi, \pi]^2$. To reduce the problem over \mathbb{R}^2 to a family of problems over Ω , one defines for $g \in L^2(\mathbb{R}^2)$ the Floquet transform

$$(\mathcal{F}g)(\alpha, x) = e^{-i\alpha \cdot x} \sum_{n \in Z^2} g(x - n)e^{i\alpha \cdot n}, \quad \alpha \in K.$$

The sum can be considered as a Fourier series in the *quasimomentum* variable α , with values in $L^2(\Omega)$; see [14] for details.

Formally, $(\nabla + i\alpha)\mathcal{F}g = \mathcal{F}(\nabla g)$, where the gradient is with respect to the x variable. Under the mapping \mathcal{F} , the E -parallel problem (3) transforms to

$$(\nabla + i\alpha) \cdot (\nabla + i\alpha)u_\alpha + \omega^2 \rho u_\alpha = 0 \quad \text{in } \Omega, \alpha \in K, \tag{6}$$

where u_α is the Floquet transform of u . Similarly, the H -parallel problem (4) transforms to

$$(\nabla + i\alpha) \cdot M(\nabla + i\alpha)u_\alpha + \omega^2 u_\alpha = 0 \quad \text{in } \Omega, \alpha \in K. \tag{7}$$

For notational simplicity, from now on we drop the subscript α when referring to u .

Let $H^1(\Omega)$ denote the usual Sobolev space of square integrable functions with square integrable first-order derivatives. The natural variational eigenproblems associated with (6) and (7) are, respectively,

$$a_\alpha(1; u, v) = \omega^2 b(\rho; u, v), \quad \text{for all } v \in H^1(\Omega) \text{ (E-parallel)} \tag{8}$$

and

$$a_\alpha(M; u, v) = \omega^2 b(1; u, v), \quad \text{for all } v \in H^1(\Omega) \text{ (H-parallel)}, \tag{9}$$

where

$$a_\alpha(M; u, v) = \int_\Omega M(\nabla + i\alpha)u \cdot \overline{(\nabla + i\alpha)v}$$

$$b(\rho; u, v) = \int_\Omega \rho u \bar{v}.$$

The quadratic forms a_α and b are Hermitian.

Discrete versions of the variational problems (8), (9) are then obtained in the standard way by introducing for a given ‘‘discretization level’’ N , an approximating subspace $S_N \subset H^1(\Omega)$. Problem (8) is then replaced by the discrete problem: find nonzero $u_N \in S_N$ and ω^2 such that

$$a_\alpha(1; u_N, \phi) = \omega^2 b(\rho; u_N, \phi), \quad \text{for all } \phi \in S_N, \tag{10}$$

and similarly for the H -parallel polarization case (9).

In our implementation, due to the simple geometry of the domain Ω , and our wish to maintain as much symmetry as possible in the discrete problem, we choose S_N to be composed of piecewise-bilinear nodal finite elements on a uniform $\sqrt{N} \times \sqrt{N}$ square grid. Convergence properties for finite element approximations for similar elliptic eigenvalue problems are well known, see, for example, [4]. For both problems (8) and (9), the finite element approximations are convergent, assuming only that ϵ is bounded, measurable, and uniformly bounded away from zero. However, for problem (8), the convergence is generally faster, essentially due to the better smoothness properties of eigenvectors u . Our focus here is not on the convergence of the discrete approximations u_N as $N \rightarrow \infty$, although some numerical examples are given in Subsection 5.2.

Given the standard set of nodal basis elements $\{\phi_j\}_{j=1}^N \subset S_N$, we write (10) as a matrix eigenproblem

$$A_\alpha^E u = \omega^2 B^E u \quad \text{(E-parallel)}, \tag{11}$$

where the entries of the matrices are given by

$$(A_\alpha^E)_{jk} = a_\alpha(1; \phi_j, \phi_k), \quad (B^E)_{jk} = b(\rho; \phi_j, \phi_k), \quad 1 \leq j, k \leq N,$$

and now u is a vector representing the approximate eigenfunction in terms of the basis $\{\phi_j\}$. The matrix problem corresponding to the H -parallel case (9) will be written

$$A_\alpha^H u = \omega^2 B^H u \quad (H\text{-parallel}), \quad (12)$$

where

$$(A_\alpha^H)_{jk} = a_\alpha(M; \phi_j, \phi_k), \quad (B^H)_{jk} = b(1; \phi_j, \phi_k), \quad 1 \leq j, k \leq N.$$

In our implementation, the integrals $b(\rho; \phi_j, \phi_k)$ and $a_\alpha(M; \phi_j, \phi_k)$ are calculated explicitly by assuming that ρ and M are piecewise constant over the grid.

3. PRECONDITIONER

Due to the periodic geometry, the differential operator

$$L_\alpha = -(\nabla + i\alpha) \cdot (\nabla + i\alpha) = -\Delta - 2i\alpha \cdot \nabla + |\alpha|^2$$

is easily separable in terms of Fourier coefficients. Specifically, writing

$$f(x) = \sum_{n \in \Lambda} f_n e^{2\pi i n \cdot x}, \quad \text{where } f_n = \int_{\Omega} f(x) e^{-2\pi i n \cdot x} dx,$$

we see that

$$L_\alpha f = \sum_{n \in \Lambda} |2\pi n + \alpha|^2 f_n e^{2\pi i n \cdot x}, \quad (13)$$

where the sum is interpreted in a weak sense if necessary. Note that for $\alpha \in K = [-\pi, \pi]^2$, the term $|2\pi n + \alpha|$ is zero only when $n = \alpha = 0$. Consequently, one has an explicit representation for the inverse (modulo constants in the $\alpha = 0$ case),

$$L_\alpha^{-1} f = \sum_{\substack{n \in \Lambda \\ 2\pi n + \alpha \neq 0}} |2\pi n + \alpha|^{-2} f_n e^{2\pi i n \cdot x}. \quad (14)$$

Our approach uses this representation to obtain a preconditioner, i.e., an approximate inverse, for the finite element discretization described in the previous section. In the discrete setting, an approximation to L_α^{-1} can be calculated very efficiently using the fast Fourier transform. Specifically, if F denotes the FFT operation on a sampled grid function on a $\sqrt{N} \times \sqrt{N}$ uniform grid, we can define

$$S_\alpha = F^{-1} D_\alpha F,$$

where D_α is a diagonal scaling matrix with entries $|2\pi n + \alpha|^{-2}$ on the diagonal. S_α can be viewed as a discrete approximation to L_α^{-1} . Since S_α is not constructed in the same finite element space as the matrix A_α^E , it will not be an exact matrix inverse. For our purposes, S_α will be used only as an *approximate* inverse for the matrix A_α^E (as well as for A_α^H). Notice that calculating the product $S_\alpha v$, for any N -vector v , is a $\mathcal{O}(N \log N)$ operation.

4. SUBSPACE PRECONDITIONING ALGORITHM

The algorithm we propose for solving the matrix eigenvalue problems (11) and (12) is a trivial modification of a method studied by Bramble, Pasciak, and Knyazev [3] (the modification is to handle generalized eigenproblems). The idea of using preconditioned iterations for computing eigenvalues is not new, dating back at least to Samokish [16] and Petryshyn [15]. Convergence analysis in the case of one eigenvalue was done by Godunov *et al.* [11]. The basic iteration used here was studied by D'yakonov and Orekhov [6]. In addition, several alternative preconditioned schemes have since been proposed to further enhance the convergence of the basic iteration; see the references in [3] for details.

Let us denote problems (11) and (12) generically by

$$A_\alpha u = \lambda B u.$$

The preconditioned subspace iteration algorithm is intended to find a relatively small number, say s , of the smallest eigenvalues in large-dimensional symmetric positive definite matrix problems. The basic method develops a sequence of approximating eigenspaces

$$V_s^n = \text{span}\{v_1, \dots, v_s\}, \quad n = 1, 2, \dots$$

Applied to our band structure calculation problem, the method proceeds as follows. First, choose an initial subspace V_s^0 . A space spanned by s pseudo-random, linearly independent N -vectors usually suffices. Next, for $n = 0, 1, 2, \dots$, perform the iteration:

(1) Compute the Ritz eigenvectors $\{v_j^n\}_{j=1}^s \subset V_s^n$, and their corresponding eigenvalues $\lambda_1^n \leq \lambda_2^n \leq \dots \leq \lambda_s^n$ satisfying

$$\langle A_\alpha v_j^n, w \rangle = \lambda_j^n \langle B v_j^n, w \rangle, \quad \text{for all } w \in V_s^n.$$

(2) Compute

$$\hat{v}_j^{n+1} = v_j^n - S_\alpha (A_\alpha v_j^n - \lambda_j^n B v_j^n), \quad \text{for } j = 1, \dots, s.$$

(3) Define $V_s^{n+1} = \text{span}\{\hat{v}_1^{n+1}, \dots, \hat{v}_s^{n+1}\}$.

Most of the work in each iteration is expended computing the matrix-vector products $A_\alpha v_j^n, B v_j^n, j = 1, \dots, s$. With the finite element discretization described Section 2, A_α and B essentially have only nine nonzero diagonals, so each matrix-vector product is an $O(N)$ operation. Computing the action of the preconditioner S_α on a vector is an $O(N \log N)$ operation. Thus with s fixed, each iteration of steps (1)–(3) requires $O(N \log N)$ time. It is important to note that the Ritz eigenproblem in step (1) is s -dimensional, so that for small s (typically $s \approx 10$), this is a trivial amount of work. The iteration (1)–(3) can be terminated, for example, when $\max_j \{|\lambda_j^n - \lambda_j^{n+1}|\}$ is less than some desired tolerance.

Estimates which, under certain assumptions on the preconditioner, prove that the subspace iteration converges at a rate which is *independent of the grid size* are provided in [3]. In the next section we will investigate numerically some of the convergence properties of the algorithm.

To do a full band structure calculation, one can now proceed in the obvious way, sampling quasimomentum vectors α in the first Brillouin zone with a finite number of α_k , and solving

each eigenproblem with the algorithm above, one k at a time. In practice, by choosing the sequence $\{\alpha_k\}$ so that each distance $|\alpha_k - \alpha_{k+1}|$ is small, one gets a good approximate subspace V_s^0 for the $(k + 1)$ st problem by using the final subspace V_s^n from the k th problem. Typically after the first problem is solved, each additional problem requires only a few subspace preconditioning iterations.

5. NUMERICAL EXPERIMENTS

Our goal in this section is to illustrate the performance of the method for typical 2D photonic crystals. The method was implemented entirely in *Matlab*; computations were carried out on a Sun UltraSparc workstation. We begin this section by presenting two simple band structure calculations.

5.1. EXAMPLES. A typical band structure calculation proceeds by computing the first s eigenvalues for various values of α , as α is varied along lines between points of high symmetry in the first Brillouin zone, as shown in Fig. 1. Alternatively, a density of states calculation can be done by sampling many values of α in the first Brillouin zone and counting corresponding states in specified frequency ranges. A simple band calculation example is shown in Fig. 2. In this example, the photonic crystal is an array of circular isotropic rods, as pictured in Fig. 2a. The rods have high dielectric constant ($\epsilon = 8.9$) and are surrounded by air ($\epsilon = 1$). Band structures in E - and H -parallel polarization modes are shown in Figs. 2b and 2c, respectively. The computations were carried out on a 64×64 grid and required roughly a half-hour of wall-clock time.

In the next example, we consider anisotropic media. As is well known, this situation arises naturally when considering “layered” composite structures, such as the one pictured in Fig. 3a. Such structures would of course be of most interest at larger-than-optical length scales, where fabrication is more plausible. In the figure, light areas represent an isotropic material with $\epsilon = 17$ and dark areas represent an isotropic material with $\epsilon = 1$. One could of course retain the isotropic problem and compute directly with the structure in Fig. 3a. However, if one wishes to increase the number of layers in each “slab” while holding its

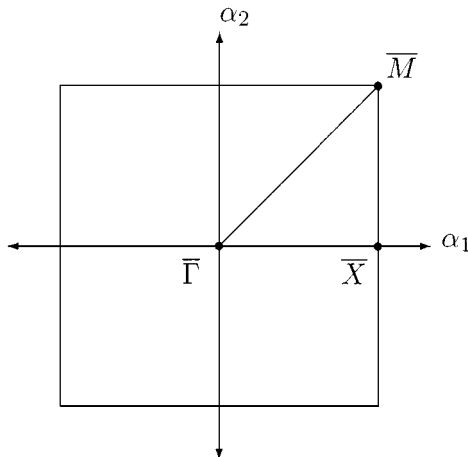


FIG. 1. First Brillouin zone and symmetry points $\bar{\Gamma}$, \bar{X} , and \bar{M} .

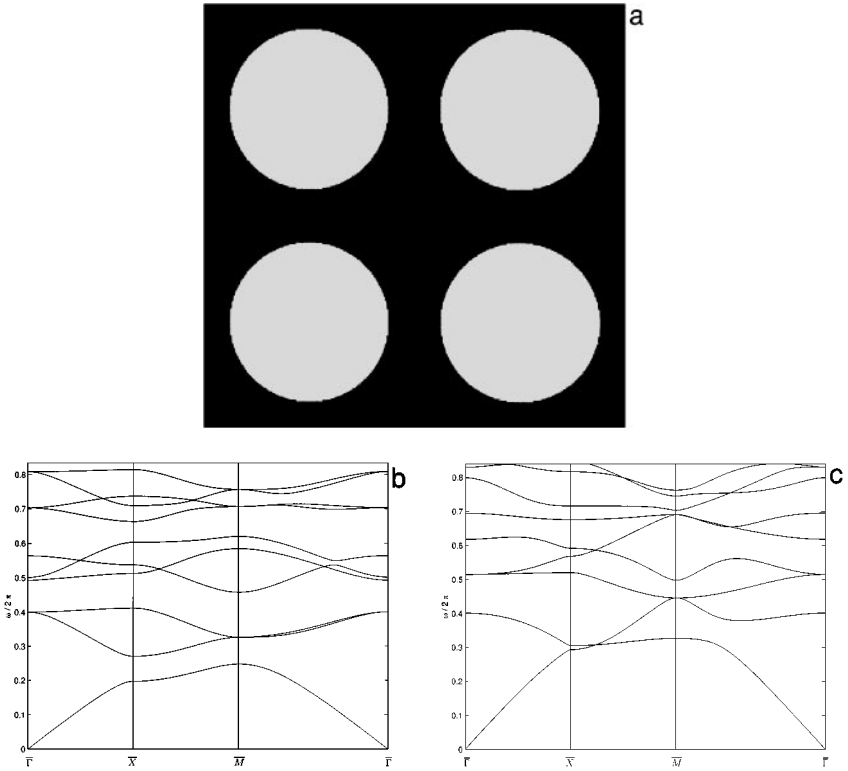


FIG. 2. Computed band structure for circular dielectric rod of radius 0.378, where the cell side length is one. (a) Four cells of circular rod structure. Light-shaded area represents $\epsilon = 8.9$; dark area has $\epsilon = 1$. (b) E -parallel polarization. (c) H -parallel polarization.

thickness fixed, then the grid must be refined, which can become a computational burden. By instead passing to the limit as the number of layers becomes infinite and applying effective media theory, one obtains an orthotropic problem. In the effective orthotropic problem, each vertical slab becomes a homogeneous composite material with

$$\epsilon = \begin{pmatrix} 9 & 0 & 0 \\ 0 & \frac{17}{9} & 0 \\ 0 & 0 & 9 \end{pmatrix}.$$

Similarly, each horizontal slab is homogeneous, with ϵ as above, but with ϵ_{11} and ϵ_{22} reversed. The band structure corresponding to this effective media model was calculated on a 64×64 grid and is shown in Figs. 3b and 3c. It was found to differ very little from the band structure obtained by direct computation on the layered isotropic model with a finer grid.

5.2. Convergence of finite element approximations. In the E -parallel case, standard convergence estimates (see, e.g., [4]) indicate that finite element solutions, using piecewise bilinear elements as in our implementation, are linearly convergent to exact solutions as the grid spacing is reduced. A numerical check of this estimate is shown in Fig. 5, where we plot the maximum difference between the first five eigenvalues, computed on $m \times m$ and $\frac{m}{2} \times \frac{m}{2}$ grids. This check is carried out on two different photonic crystals: the

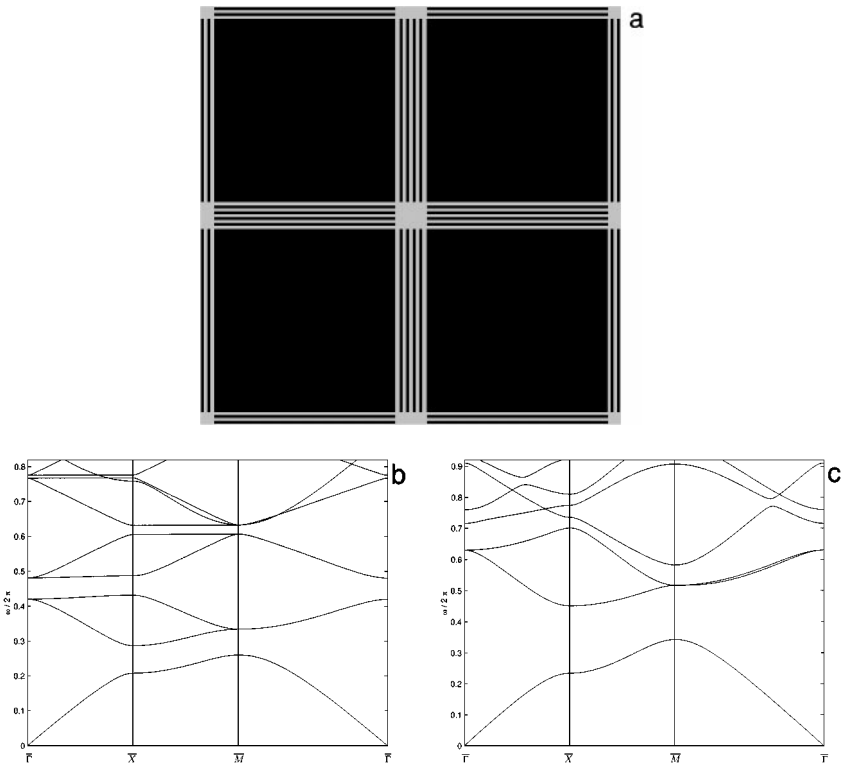


FIG. 3. Computed band structure for (anisotropic) effective medium limit of layered structure. Note that gaps appear in both E - and H -parallel modes. (a) Four cells of layered structure. Light-shaded area represents $\epsilon = 17$; dark area has $\epsilon = 1$. (b) E -parallel polarization. (c) H -parallel polarization.

first is the circular dielectric rod structure shown in Fig. 2a, and the second is a similar dielectric rod structure with a square cross section and side length 0.5, shown in Fig. 4. The computational results are consistent with linear convergence in both cases, and also agree with the type of convergence behavior observed by Axmann and Kuchment

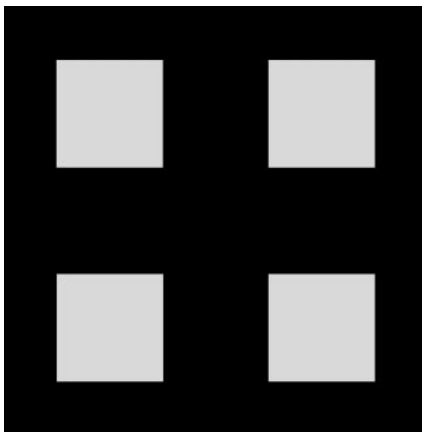


FIG. 4. Square rod structure used for convergence checks. Rod side length is 0.5, dielectric coefficient in rod (shaded light) is $\epsilon = 8.9$, and surrounding medium is $\epsilon = 1$.

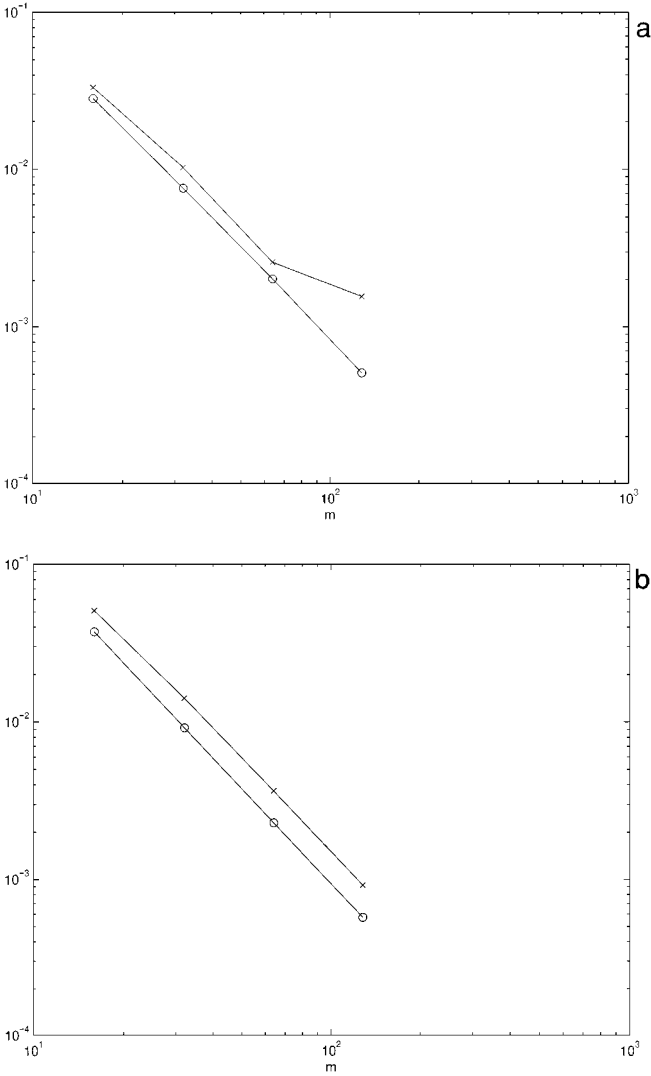


FIG. 5. Maximum difference in first five computed eigenvalues $\max_j |\lambda_j^m - \lambda_j^{m/2}|$, where λ_j^m is the j th eigenvalue computed on an $m \times m$ grid, versus linear grid size m . Circles indicate E -parallel mode; crosses indicate H -parallel mode. (a) Circular dielectric rod structure. (b) Square dielectric rod structure.

[1]. In H -parallel polarization, it can be proved that the finite element approximation is convergent, but for arbitrary $\epsilon(x)$ one cannot expect a definite convergence rate. In Fig. 5a we see that convergence in H -parallel mode appears to be less than linear for the circular dielectric rod structure. Some improvement could be obtained by implementing more accurate integration rules; recall from Section 2 that in our implementation, the matrix entries (12) are calculated assuming a piecewise constant dielectric coefficient. For structures in which jumps in the dielectric coefficient are aligned with the computational grid, as in the square rod example, the integration rules are exact and the grid conforms naturally with the regularity of the eigenfunctions. Consequently, convergence is better, as shown in Fig. 5b.

5.3. Convergence of subspace iterations. In practice, the number of preconditioned subspace iterations required to reach a given tolerance in $\max_j \{|\lambda_j^n - \lambda_j^{n+1}|\}$ is at worst a

very slowly growing function of the grid size N . This is difficult to check numerically, because a primary factor determining the number of iterations required on a subspace of a given dimension s is the distance between the largest eigenvalue λ_s within the subspace and the smallest eigenvalue λ_{s+1} outside the subspace. As N is varied, this distance generally changes. However, for simple examples chosen such that $|\lambda_s - \lambda_{s+1}|$ is relatively insensitive to N , we can get a qualitative idea of the general behavior. For a series of computations in which the first three bands in E -parallel polarization of the square rod structure shown in Fig. 4 were calculated to a stopping tolerance of $\max_j \{|\lambda_j^n - \lambda_j^{n+1}|\} < 5 \times 10^{-6}$, the average number of subspace iterations per solve grows monotonically, but slowly, from 5.7 iterations for $N = 256$ to 6.1 iterations at $N = 16384$. Furthermore, as illustrated in Fig. 6a, the amount of work required for the complete band calculation (measured in number of

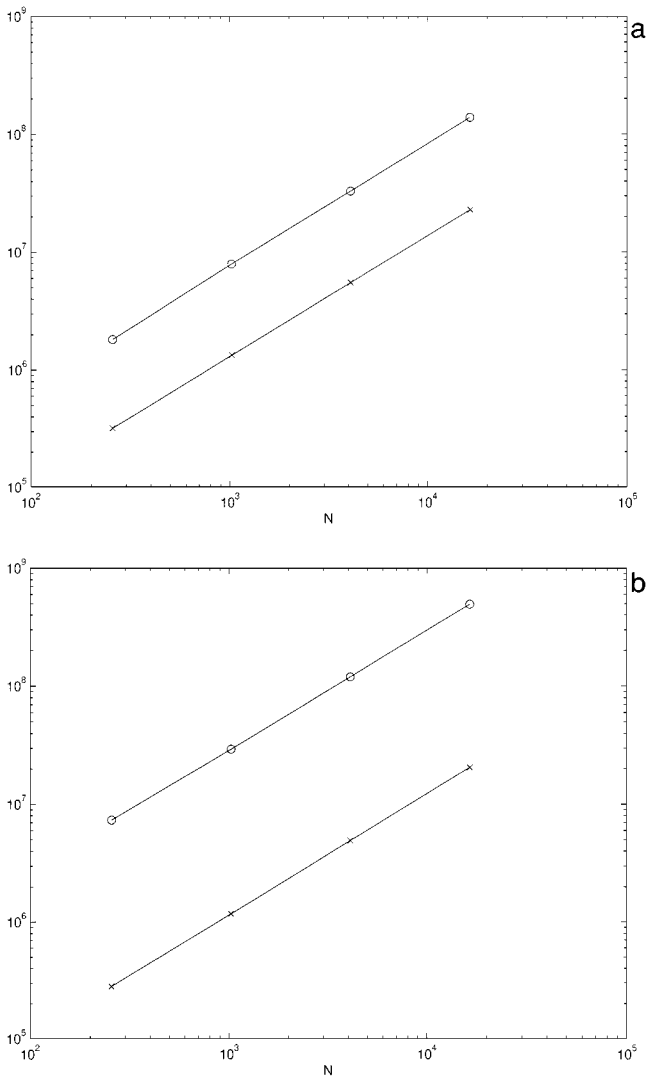


FIG. 6. Number of floating point operations versus grid size N . Circles represent average number of operations per solve. Crosses represent average number of operations per preconditioned subspace iteration. (a) E -parallel polarization example. (b) H -parallel polarization example.

floating point operations) scales roughly like $N \log N$, the same as a single preconditioned subspace iteration.

The preconditioner is generally not as effective in the H -parallel polarization case as it is in E -parallel polarization. Hence each solve requires more subspace iterations. In a series of computations similar to the last example, but in H -parallel polarization, the average number of subspace iterations per solve was larger, but actually decreased monotonically from 26.1 iterations per solve at $N = 256$, to 24.1 iterations per solve at $N = 16384$. Average work per solve and per step increased “almost” linearly with N , as illustrated in Fig. 6b.

A key factor determining the effectiveness of the preconditioner is the contrast between dielectric coefficients of the materials which compose the photonic crystal. Generally, the preconditioner works better for small contrast. The effect of the preconditioner on convergence of the subspace iteration is complicated, but can be examined qualitatively by looking

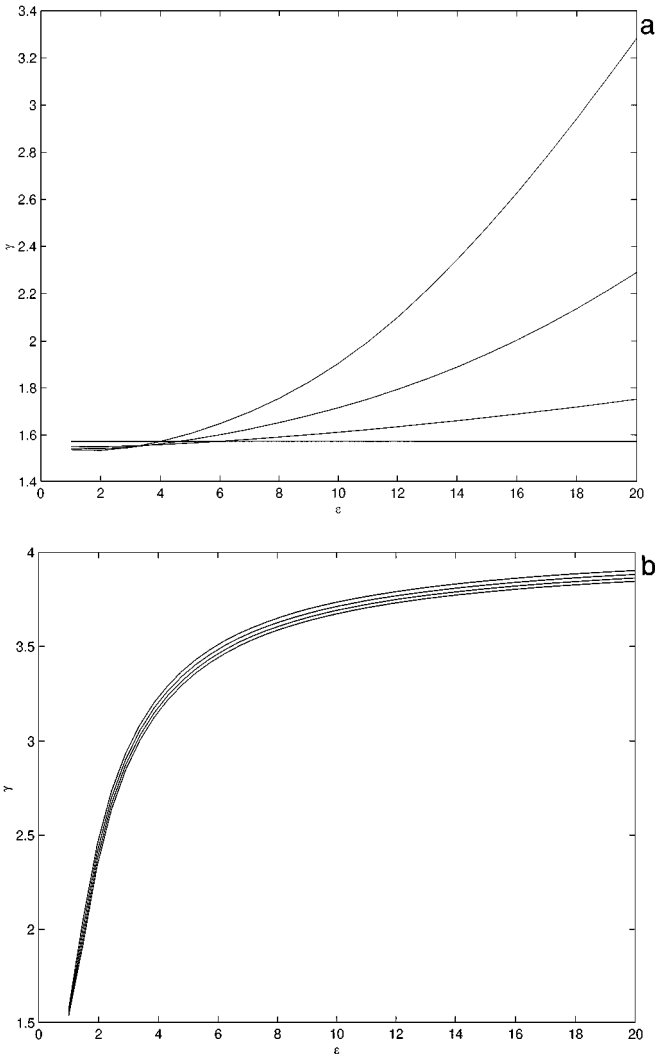


FIG. 7. The quantity $\gamma(\lambda)$, defined in (15), for $\lambda = 0, \frac{1}{3}, \frac{2}{3}, 1$. The horizontal axis represents the contrast in material parameters for the isotropic dielectric rod structure in Fig. 2. (a) E -parallel polarization. (b) H -parallel polarization.

at the step

$$\hat{v}_j^{n+1} = v_j^n - S_\alpha (A_\alpha v_j^n - \lambda_j^n B v_j^n).$$

Roughly speaking, if the quantity

$$\gamma(\lambda) = \|S_\alpha(A_\alpha - \lambda B)\|, \quad (15)$$

is small, then the update to the approximate eigenvector \hat{v}_j^{n+1} is small, and the iteration converges more rapidly. The behavior of $\gamma(\lambda)$ is different for E - and H -parallel modes, but always increases with the contrast. Figure 7 shows various values of $\gamma(\lambda)$ as the contrast of the dielectric rod structure is increased from $\epsilon = 1$ to $\epsilon = 20$. Obviously the E -parallel mode behaves better in the optical contrast range $\epsilon \approx 9$. This helps explain the improved convergence we observed in E -parallel mode in the numerical examples. Note however that the H -parallel mode appears to have better asymptotic behavior for large contrast.

6. CONCLUSIONS

We have presented an efficient method for performing band structure calculations in “two-dimensional” photonic crystals. The method uses a finite element discretization coupled with a preconditioned subspace iteration algorithm to solve the discrete eigenproblems. The method can be applied to very general dielectric structures, including those with anisotropic media. The method is most efficient for photonic crystals composed of low-contrast media. Numerical experiments indicate that the computational work required per solve is $\mathcal{O}(N \log N)$, where N is the number of points in the discretization. The basic approach can in principle be extended to handle three-dimensional structures, and more general periodic geometries.

ACKNOWLEDGMENTS

The author thanks W. Axmann and P. Kuchment for several helpful discussions. Acknowledgment and Disclaimer: Effort sponsored by the Air Force Office of Scientific Research, Air Force Materiel Command, USAF, under Grant F49620-98-1-0005. The U.S. Government is authorized to reproduce and distribute reprints for Governmental purposes notwithstanding any copyright notation thereon. The views and conclusions contained herein are those of the authors and should not be interpreted as necessarily representing the official policies or endorsements, either expressed or implied, of the Air Force Office of Scientific Research or the U.S. Government.

REFERENCES

1. W. Axmann and P. Kuchment, A finite element method for computing spectra of photonic and acoustic band-gap materials. I. Scalar case, preprint, 1998.
2. C. M. Bowden, J. P. Dowling, and H. O. Everitt, editors, Development and applications of materials exhibiting photonic band gaps, *J. Opt. Soc. Amer. B* **10**(2), (1993).
3. J. H. Bramble, A. V. Knyazev, and J. E. Pasciak, A subspace preconditioning algorithm for eigenvector/eigenvalue computation, *Adv. Comput. Math.* **6**, 159 (1996).
4. P. G. Ciarlet, *The Finite Element Method for Elliptic Problems* (Elsevier North-Holland, Amsterdam, 1978).
5. S. J. Cox and D. C. Dobson, Maximizing band gaps in two-dimensional photonic crystals, *SIAM J. Appl. Math.*, in press.

6. E. G. D'yakonov and M. Yu. Orekhov, Minimization of the computational labor in determining the first eigenvalues of differential operators, *Math. Notes* **27**, 382 (1980).
7. J. M. Elson and P. Tran, Coupled-mode calculation with the R-matrix propagator for the dispersion of surface waves on a truncated photonic crystal, *Phys. Rev. B* **54**(3), 1711 (1996).
8. A. Figotin and Y. A. Godin, The computation of spectra of some 2D photonic crystals, *J. Comput. Phys.* **136**, 585 (1997).
9. A. Figotin and P. Kuchment, Band-gap structure of spectra of periodic dielectric and acoustic media. I. Scalar model, *SIAM J. Appl. Math.* **56**, 68 (1996).
10. A. Figotin and P. Kuchment, Band-gap structure of spectra of periodic dielectric and acoustic media. II. Two-dimensional photonic crystals, *SIAM J. Appl. Math.* **56**, 1561 (1996).
11. S. K. Godunov, V. V. Ogneva, and G. P. Prokopov, On the convergence of the modified steepest descent method in application to eigenvalue problems, *Trans. Amer. Math. Soc.* **2**, 105 (1976).
12. J. Jin, *The Finite Element Method in Electromagnetics* (Wiley, New York, 1993).
13. J. D. Joannopoulos, R. D. Meade, and J. N. Winn, *Photonic Crystals: Molding the Flow of Light* (Princeton Univ. Press, Princeton, NJ, 1995).
14. P. Kuchment, *Floquet Theory for Partial Differential Equations* (Birkhäuser, Basel, 1993).
15. W. V. Petryshyn, On the eigenvalue problem $Tu - \lambda Su = 0$ with unbounded and non-symmetric operators T and S , *Philos. Trans. Roy. Soc. Math. Phys. Sci.* **262**, 413 (1968).
16. B. A. Samokish, The steepest descent method for an eigenvalue problem with semi-bounded operators, *Izv. Vyssh. Uchebn. Zaved. Mat.* **5**, 105 (1958). [In Russian]